A Sensorless Control Strategy for IPMSM based Electric Power Steering Systems

GIACOMO SCELBA**, SALVATORE DE CARO*, ANTONIO TESTA*, GIUSEPPE SCARCELLA**, MARIO CACCIATO**

* Department Electronic Engineering, Industrial Chemistry and Engineering
University of Messina,
Contrada Di Dio – 98166 Messina (ME)
ITALY
sdecaro@unime.it , atesta@unime.it

** Department of Electrical, electronics and computer science
University of Catania,
Viale Andrea Doria – 95125 Catania,
ITALY
giacomo.scelba@dieei.unict.it , giuseppe.scarcella@dieei.unict.it , mario.cacciato@dieei.unict.it

Abstract: - Electric power steering systems are a quite common equipment of modern vehicles. They are based on torque controlled electromechanical actuators assisting the driver in moving the steering wheel. These systems must generate low torque fluctuations and mechanical vibrations, while featuring a low cost and a simple and rugged control system. In order to comply with these requirements an electromechanical actuator based on a sensorless controlled synchronous motor is proposed in this paper. It exploits a sensorless torque control technique based on the injection of high frequency voltage signals and the manipulation of induced high frequency stator current components. A key feature of this technique is a very simple implementation using a low cost mixed (analog/digital) circuitry, requiring a minimal computational power. Implementation issues and experimental results obtained on a laboratory prototype, based on a standard electric power steering system, are presented to confirm the consistence of the proposed approach.

Key-Words: - Sensorless Control; Electric Power Steering systems (EPS); Automotive; Interior Permanent Magnet Synchronous Machine (IPMSM);

1 Introduction

Electric Power Steering (EPS) is today a standard equipment even on low end vehicles, providing better steering feel and higher degrees of adaptability and efficiency in comparison with Hydraulic and Electro-Hydraulic systems [1], [2]. Moreover, traditional components of hydraulic devices, such as pumps, fluids, hoses, pulleys and drive-belts can be eliminated, thus simplifying the design and manufacturing of the steering system [3]. Finally, operations of the EPS and the car engine are made independent, increasing the efficiency and allowing steering assistance even if the engine is off.

An EPS system is basically composed of a torque commanded electric motor drive acting on the steering column. It is tasked to assist the steering by generating a smooth torque on the rack, whilst also providing a sort of torque feedback to the driver. The reference motor torque is determined by a control unit on the basis of the torque applied by the driver to the steering wheel, the angular speed of the steering wheel, the steering angle and the vehicle speed. Different electrical machines can be considered to equip an EPS system, such as PM DC motors, DC Brushless motors, Switched Reluctance motors, Surface Mounted and Interior PM motors. Among them, the Permanent Magnet DC motor is today the most widely used, due to the easy driving and a mature and well accepted technology. However, some alternative solutions have been recently proposed in an attempt to reduce vibrations and torque fluctuations, that are directly transferred through the steering wheel to the hands of the driver. Specifically, in order to contain torque fluctuations above 1~3% of rated torque the Interior Permanent Magnet Synchronous Machine (IPMSM) has been considered. Such an electric motor ensures the highest levels of torque density, thanks to its additional reluctance torque, high efficiency and

compactness. Moreover, among electrical machines used in power steering systems it is able to generate the highest torque at standstill, and shows a very small torque fluctuation, leading to very low mechanical vibration and noise.
However, compared with a DC or a Brushless DC machine an IPMSM needs a more complex vector control algorithm requiring extra position sensors such as resolvers or optical encoders. Unfortunately, in power steering applications position sensors not only decrease the reliability of the whole system (due to an harsh operational environment), but also partially vanish the advantages of IPMSMs in terms of compactness and torque density, as extra space and suitable mounting arrangements are required.
A possible solution to make IPMSMs more viable to replace DC and Brushless DC machines in EPS systems consists in the elimination of the position sensor, by exploitation of a position sensorless control technique [4]. Several sensorless techniques have been proposed in the past, however, some specific requirements must be taken into major account when dealing with EPS applications, such as:

• Implementation costs

• Algorithm complexity (to enable the use of low cost microcontrollers with few memory)

• Accuracy, either at steady state, either during transients

• Low- and zero-speed working capabilities

• Robustness to motor parameter and load variations

These requirements are fully complied by the simple sensorless control technique proposed in this paper, based on the injection of a high frequency voltage test signal and the measurement of the machine current response. Such a technique does not require the knowledge of any motor parameter, or particular procedures when starting the motor from an unknown position, it is able to drive an IPMSM at any load, even at low and zero speed. Even the theoretical background of the proposed sensorless technique is common to other signal injection approaches exploiting the anisotropy of the machine to accomplish an estimation of the rotor angular position [5]÷[8], it allows a very simple implementation, enabling a low-cost practical realization, and is robust to the effects of saturation, cross coupling and motor parameter variations.

Moreover, a torque sensor is required to command the EPS drive. It is generally obtained by a differential position transducer measuring the deformation of a segment of the steering column of known stiffness. Using the proposed sensorless technique to estimate the angular position of one end of the steering column, only a simple position transducer placed on the other end of the steering column is required to measure the torque applied to the steering wheel.

2 Signal injection based rotor position estimation

A robust sensorless estimation of the shaft position can be obtained on PM machines featuring a rotor saliency by adding a low-amplitude, high-frequency (fhf >500 Hz) rotating voltage vector to the normal stator voltage. The additional voltage component produces a zero average torque and a negligible torque ripple, but, due to the rotor saliency, it generates a stator current component whose amplitude is function of the mutual position between the rotating vector and the rotor [5]. In fact, as shown in Fig. 1, in a IPMSM the stator impedance at the frequency of the injected voltage is spatially modulated due to the anisotropy of the rotor structure.

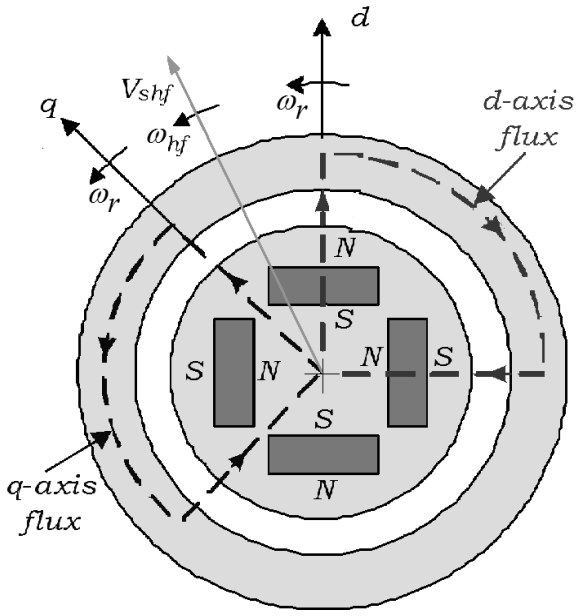

Fig. 1 - IPMSM rotor structure and vector diagram.

More precisely, the rotor q axis direction features the highest level of impedance, because the q axis flux path takes place almost entirely inside the

ferromagnetic core, where the reluctance is quite low. On the other hand, the lowest impedance level is found along the d-axis, where the flux path crosses the permanent magnets leading to a high reluctance.
Due to the spatial stator impedance modulation, the amplitude of the current vector , generated by the voltage vector is influenced by the angular displacement between and the rotor q axis. More precisely, as the rotating vector travels at a higher angular speed than the rotor, a minimum of the amplitude of periodically occurs whenever the injected voltage vector is spatially aligned with the maximum inductance axis (q axis) and a maximum occurs whenever is spatially aligned with the minimum inductance axis (d axis). By analyzing the sequence of maximum and minimum points of the amplitude of , it is easy to identify the absolute position of the rotor q and d axes from the known position of the rotating vector. Having detected the position of the d, q rotor axes the correct orientation of the two axes can be determined by a suitable initialization procedure, as common in all the sensorless rotor position estimation techniques exploiting the machine anisotropy.
In the following the theoretical development of the proposed technique is first presented, then practical implementation issues will be discussed.

2.1 Theoretical background

By neglecting hysteresis and eddy current losses the model of a cageless IPMSM, written in the d-q reference frame synchronous with the rotor, is:

$$v_{qs} = r_s i_{qs} + \frac{d\lambda_{qs}}{dt} + \omega_r \lambda_{ds} \tag{1}$$

$$v_{ds} = r_s i_{ds} + \frac{d\lambda_{ds}}{dt} - \omega_r \lambda_{qs} \tag{2}$$

$$\frac{d\omega_r}{dt} = \frac{1}{J}\left(T_e - T_l\right) \tag{3}$$

$$\lambda_{qs} = L_q i_{qs} = \left(L_{ls} + L_{mq}\right) i_{qs} \tag{4}$$

$$\lambda_{ds} = L_d i_{ds} + \lambda_{PM} = \left(L_{ls} + L_{md}\right) i_{ds} + \lambda_{PM} \tag{5}$$

$$T_e = \frac{3}{2} pp\left(\lambda_{MP} I_s \sin(\varepsilon\varepsilon + (L_{md} - L_{mq}) I_s^2 \frac{\sin(2\varepsilon)}{2} \right) \tag{6}$$

being $\varepsilon = tan^{-1}(i_{ds}/i_{qs})$, moreover, according to Fig. 1 it is assumed that $L_{md} < L_{mq}$

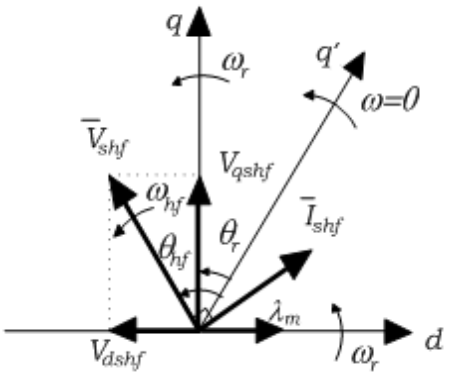

Fig. 2 - Synchronous reference frame and rotating vectors.

Considering the IPMSM supplied only with the additional high frequency voltage Vshf and forced to rotate at low speed by another machine, according to Figs. 1 and 2, the mathematical model of the machine in the d, q rotor reference frame gives :

$$V_{shf}\cos\left(\theta_{hf} - \theta_r\right) = r_{shf} i_{qshf} + \omega_r \left(L_{dshf} i_{dshf} + \lambda_{PM}\right) + L_{qshf} \frac{di_{qshf}}{dt} \tag{7}$$

$$-V_{shf}\sin\left(\theta_{hf} - \theta_r\right) = r_{shf} i_{dshf} - \omega_r L_{qshf} i_{qshf} + L_{dshf} \frac{di_{dshf}}{dt} \tag{8}$$

where, R_{shf}, L_{dshf} and L_{qshf} are respectively, the stator winding resistance and the stator inductances at the frequency of the additional voltage vector $\vec{V}_{shf}$.

Moreover:

$$\theta_r = \int_0^t \omega_r dt + \theta_{ro} \tag{9}$$

$$\theta_{hf} = \int_0^t \omega_{hf} dt + \theta_{hfo} \tag{10}$$

are the absolute angular positions of the rotor q-axis and of the additional rotating voltage vector $\vec{V}_{shf}$, according to a d', q' stationary reference frame. Due to the high frequency of the injected signal the stator

resistance can be neglected if compared with the reactance [4], [7], therefore, the high frequency impedance of the machine can be considered purely inductive. Assuming, the speed of the machine sufficiently low if compared with ω_{hf}, rotational terms proportional to ω_r can be also neglected, giving:

$$V_{shf}\cos\left(\theta_{hf}-\theta_r\right)=L_{qshf}\frac{di_{qshf}}{dt} \tag{11}$$

$$-V_{shf}\sin\left(\theta_{hf}-\theta_r\right)=L_{dshf}\frac{di_{dshf}}{dt} \tag{12}$$

Solving (11) and (12), the following expressions are obtained:

$$i_{dshf}=\frac{-\sin\left(\theta_{hf}-\theta_r\right)}{\left(\omega_{hf}-\omega_r\right)L_{dshf}}V_{shf} \tag{13}$$

$$i_{qshf}=\frac{\cos\left(\theta_{hf}-\theta_r\right)}{\left(\omega_{hf}-\omega_r\right)L_{qshf}}V_{shf} \tag{14}$$

The squared amplitude of the current vector $\vec{I}_{shf}$ is then given by:

$$\begin{aligned}I_{shf}^2(t)&=i_{dhf}^{\ 2}+i_{qhf}^{\ 2}=\bar{I}_{shf}^{\ 2}+\tilde{I}_{shf}^{\ 2}\\&=\left(\frac{V_{shf}}{\left(\omega_{hf}-\omega_r\right)^2L_{dshf}L_{qshf}}\right)^2\left(\omega_{hf}-\omega_r\right)^2L_{qhf}^{\ 2}+\\&+\left(\frac{V_{shf}}{\left(\omega_{hf}-\omega_r\right)^2L_{dshf}L_{qshf}}\right)^2\left(\omega_{hf}-\omega_r\right)^2\left(L_{dhf}^{\ 2}-L_{qhf}^{\ 2}\right)\cos^2\left(\vartheta_{hf}-\vartheta_r\right)\end{aligned} \tag{15}$$

According to Eq. (15), $I_{sh}^{\ 2}$ is composed of two terms, a DC component $\bar{I}_{shf}^{\ 2}$ and an AC component $\tilde{I}_{shf}^{\ 2}$. The last, periodically reach a point of maximum when $\theta_{hf}=\theta_r$, or, in other words, when the vector $\vec{V}_{shf}$ is aligned with the q-axis and $\vec{I}_{shf}$ with the d-axis. In fact, as shown in Fig. 2, neglecting the resistive and rotational terms in Eqs. (7) and (8) the current vector $\vec{I}_{shf}$ is orthogonal to the voltage vector $\vec{V}_{shf}$. A point of minimum is, on the other hand, obtained when $\theta_{hf}=\theta_r+\pi/2$, in this case $\vec{V}_{shf}$ is aligned with the d-axis and $\vec{I}_{shf}$ with the q-axis. More generally, a maximum point of the function $\tilde{I}_{shf}^{\ 2}$ takes place if $\theta_{hf}=\theta_r\pm k\pi$ $(k=0,1,\ldots,n)$ and a minimum point if $\theta_{hf}=\theta_r+\pi/2\pm k\pi$ $(k=0,1,\ldots,n)$. This makes possible to robustly estimate the rotor position from the known position of the voltage vector $\vec{V}_{shf}$ only detecting maximum and minimum points of $\tilde{I}_{shf}^{\ 2}$.

2.1.1 Rotor position estimation

On the basis of Eq. (15), a suitable procedure can be carried out to quickly extract the rotor position θ_r. First of all a suitable circuit able to detect the occurrence of a null time derivative of $|I_{shf}|^2$ has been developed as shown in Fig. 3.

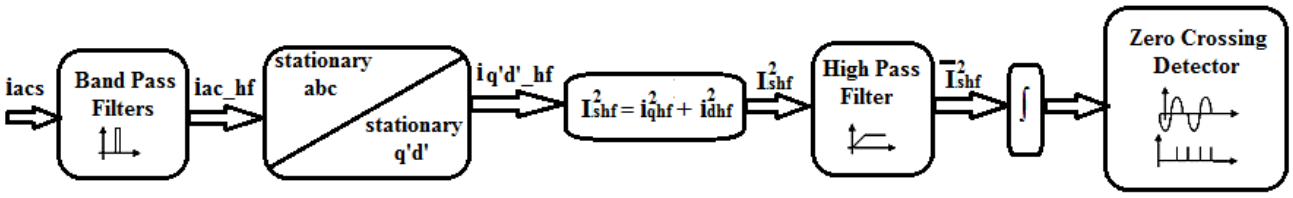

Fig. 3 - Schematic of the peak detection circuit.

High frequency components of the stator current caused by the addiction of the high frequency voltage V_{shf} are first separated from the fundamental component through suitable bandpass filters and the square of the amplitude of the current vector $\vec{I}_{shf}$ is computed. The obtained signal is then processed by mean of an high pass filter to eliminate the DC term

of Eq. (15) to obtain $\tilde{I}_{shf}^{\,2}$. In order to improve the robustness of the position estimation, rather than directly detecting maximum and minimum points of $\tilde{I}_{shf}^{\,2}$, the last is integrated and zero crossing points of the obtained signal are instead detected. No anti wind-up measures must be adopted when performing the integration, due to the high pass filters, which eliminates any DC component.
The zero crossing detector generates a sequence of pulses that are delivered to a microprocessor. Therefore, each time that a pulse is received by the microprocessor, the rotor position can be computed from the known position θ_{hf} , although with an uncertainty due to the fact that each $\tilde{I}_{shf}^{\,2}$ zero crossing, and therefore each pulse, corresponds to an alignment of the $\vec{V}_{shf}$ vector with one of the two axes.
Which is the axis and how it is oriented, positive or negative, is unknown. To solve such an uncertainty a suitable initialization procedure has been developed in order to correctly identify the position of the positive q axis at standstill, then the sequence *+q,-d,-q,+d* is assumed for the counterclockwise rotation and the sequence *+q,+d,-q,-d*, for the clockwise direction.
The direction of the movement is in turn simply obtained from the direction of the rotation impressed by the driver to the steering column, that is detected by a separated position sensor, required for torque measurement purposes. Therefore, the rotor position is determined by the microprocessor through a simple procedure according to the following rules:

$$\theta_r = \theta_{hf} \qquad \text{if } \vec{V}_{shf} \text{ is aligned with } +d$$

$$\theta_r = \theta_{hf} + \pi/2 \qquad \text{if } \vec{V}_{shf} \text{ is aligned with } -q$$

$$\theta_r = \theta_{hf} + \pi \qquad \text{if } \vec{V}_{shf} \text{ is aligned with } -d$$

$$\theta_r = \theta_{hf} + 3\pi/2 \qquad \text{if } \vec{V}_{shf} \text{ is aligned with } +q$$

According to Eq. (16), the rotor position is evaluated *4* times along each period of the $\tilde{I}_{shf}^{\,2}$ function. Consequently, the position sampling time T_s, defined as the time period between two consecutive position measurements is given by:

$$T_s = \frac{\pi}{2\left|\omega_{hf} - \omega_r\right|} \tag{17}$$

The sampling time depends on the rotor speed, and it can be minimized by forcing the additional voltage vector to rotate in the opposite direction than the rotor. As an example, using a 5*00 Hz* additional stator voltage component, T_s assumes the values reported in Tab. I for a four poles machine.

TABLE I. - ROTOR POSITION SAMPLING TIME

Rotor speed	***Ts (pp=2)***
0 rpm	*500 μs*
1000 rpm	*536 μs*
2000 rpm	*577 μs*
- 1000 rpm	*469 μs*
- 2000 rpm	*441 μs*

In normal operations the IPMS machine is not supplied only by the additional high frequency voltage as previously supposed, but, rather V_{shf} is superimposed to the fundamental stator voltage. Fundamental currents may slightly affect the location of maximum and minimum points of $\tilde{I}_{shf}^{\,2}$, due to saturation and cross-coupling effects [6]÷[9], thus influencing the position estimation. This causes a load dependence and an estimation error $\Delta\theta_e$ that can be mitigated by a suitable choice of the i_{ds} current component and, specifically, by adopting a Maximum Torque per Ampere (MTPA) control strategy [6], [8]. Therefore, driving the machine according to the MTPA approach, not only the machine efficiency is maximized, but also the estimation error $\Delta\theta_e$ is nearly minimized. Anyway, as $\Delta\theta_e$ only depends from machine design parameters, it can be predetermined by a suitable self-commissioning procedure. Then, the estimation error $\Delta\theta_e$ can be fully on-line corrected.
The accuracy of the proposed technique slightly worsens when the machine operates at high speed. In this case, in fact, due to the rotational terms of Eqs.(7) and (8) the shape of $\tilde{I}_{shf}^{\,2}$ is distorted, affecting the position estimation. However, an unacceptable distortion happens only at a relatively high speed and can be mitigated by suitably

increasing the frequency of the injected voltage component V_{shf}. Experimental results shown in this paper demonstrate that operations close to the rated speed can be easily achieved through the proposed sensorless technique.

2.1.2 Rotor position detection at standstill

Initialization of the rotor position estimation can be performed by locally inducing a variation of the saturation level in the magnetic core of the machine [10]÷[12]. The injection at standstill of a stationary current vector $\vec{I}_{s0}$ in addition to $\vec{V}_{shf}$ causes the saturation of the flux paths along the direction of $\vec{I}_{s0}$. This generates a variation of the stator inductances, that in turn affects the amplitude of $\tilde{I}_{shf}^{\,2}$. More precisely, the amplitude of $\tilde{I}_{shf}^{\,2}$ is maximum if $\vec{I}_{s0}$ is aligned with the *d* axis, as the saturation level along the *d* axis flux path is increased, thus reducing the *d* axis inductance, while it is minimum if $\vec{I}_{s0}$ is aligned with the q axis. A simple gradient descent algorithm monitoring the amplitude of $\tilde{I}_{shf}^{\,2}$ and acting on the position of $\vec{I}_{s0}$ has been developed quickly detecting the position of the d axis when turning on the ignition key. As shown in Fig 4, once the direction of the *d* axis is identified, a DC current pulse is injected along an arbitrarily supposed positive direction of the d axis. Zero torque is generated, avoiding any shaft motion but, if the injected current and the magnet flux own the same sign the saturation level will increase, the d-axis inductance will decrease and the amplitude of the high frequency current component will increase.

On the contrary, if the current and the flux have opposite signs the saturation level decreases, increasing the d-axis inductance and reducing the amplitude of $\tilde{I}_{shf}^{\,2}$. Therefore by checking at standstill the amplitude of $\tilde{I}_{shf}^{\,2}$ the correct position of the +d rotor axis can be detected to properly initialize the rotor position estimation.

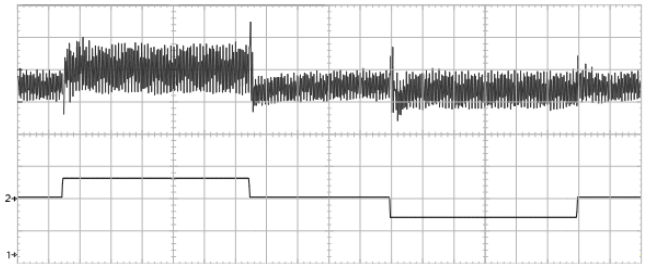

Fig. 4 - *Time = 50 ms/div;* 1) amplitude of $\tilde{I}_{shf}^{\,2}$, 5*00 mA²/div*; 2) d-axis test current, *10 A/div*.

3 Sensorless control system

According to the previously described sensorless technique, a low cost sensorless control scheme has been carried out, as shown in Fig. 5. A key feature of the proposed scheme is that the position estimation is accomplished almost entirely through an analog circuitry, minimizing the microcontroller computational effort and the memory requirements.

The first task of the analog circuit is the separation of the current feedback signals from the *500 Hz* component by suitable notch filters. The $\tilde{I}_{shf}^{\,2}$ zero crossing detection is then accomplished through five steps, namely:

- Filtering
- Computation of $\tilde{I}_{shf}^{\,2}$
- Integration
- Zero crossing detection

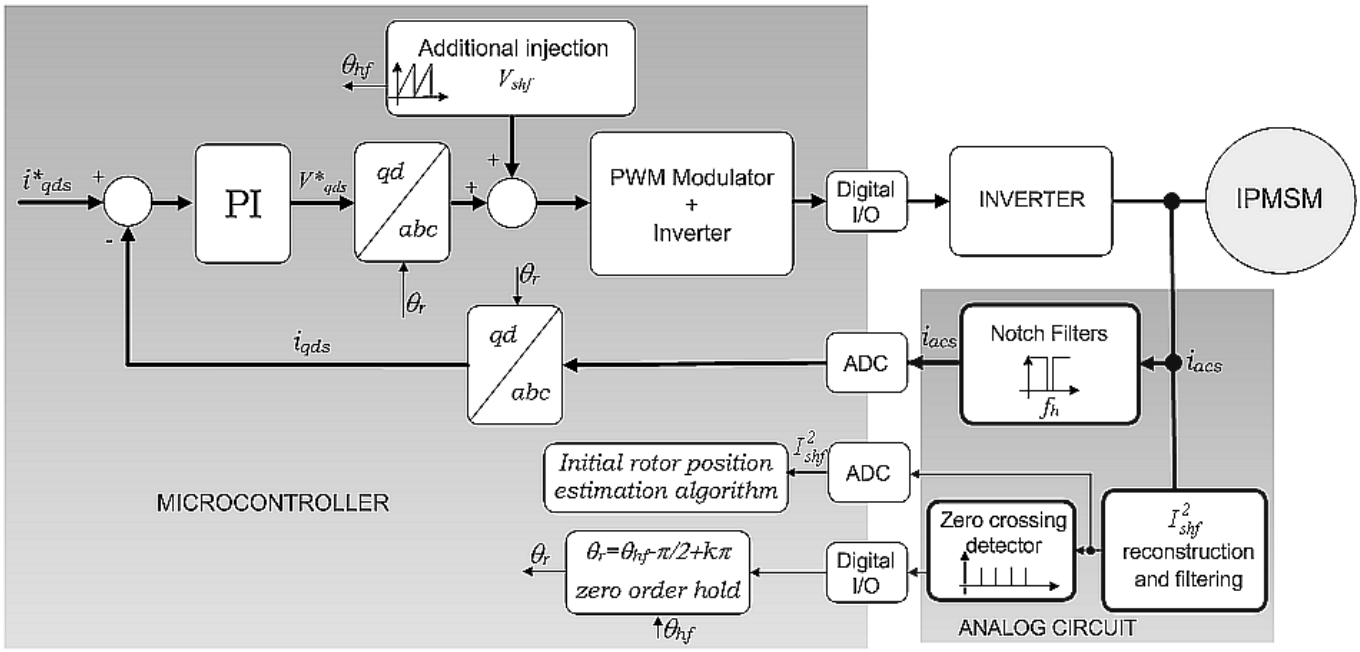

Fig. 5 - Block Diagram of the proposed sensorless technique.

According to Figs. 5, filtering is aimed to the elimination of fundamental and switching harmonic components from the current signals to be processed. It is performed by a second order Butterworth bandpass filter. A Clarke transformation is then accomplished through a fully analog circuitry to obtain the components of the high frequency current component according to a stationary *d', q'* reference frame. The signals representing $i_{q'hf}$ and $i_{d'hf}$ are also suitably amplified to increase the signal-to-noise ratio.

The function $\widetilde{I}_{shf}{}^2$ is then computed using two four quadrant analog multipliers and some operational amplifiers. An analog integrator and a voltage comparator then respectively accomplish the fourth and fifth steps. Obtained results are shown in Fig. 6.

According to Eq. (17) the frequency of the generated pulses and consequently the rotor position sampling time depends from f_{hf}. In the present case f_{hf} was set to *500Hz*, leading to a $500\mu s$ position sampling time on a four poles IPMSM at zero speed. The zero-crossing pulses are finally sent to a digital I/O port of the microcontroller and used as hardware interrupts. The microcontroller then barely computes the rotor position θ_r from known values of θ_{hf}, according to Eq. (16). Such a minimal computing power requirement opens the perspective to implement a the sensorless vector control using very low cost *8* or *16 bit* microcontrollers, working at some MHz, as those common in automotive applications.

The developed system is also able to fully accomplish the initialization procedure.

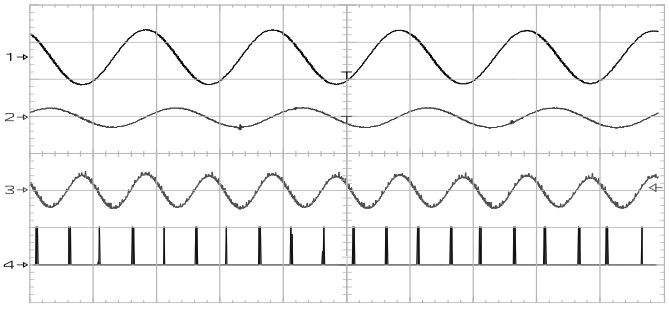

Fig. 6 - Time=*1ms/div*; 1), 2) high frequency q'-d' current components, 3) integrated $\widetilde{I}_{shf}{}^2$; 4) zero crossing pulses.

4 Sensorless control system

The proposed sensorless control approach has been tested on a 1.08 kW, 150V IPMS machine suited for robotic applications. Even the machine used for experimental tests was not specifically designed for an electric power steering application, anyway, obtained results can be fully generalized. Experimental results confirm the feasibility of the proposed approach and specifically the consistence of the analog circuit sketched in Fig. 5. The motor has been supplied by a standard three-phase IGBT

inverter. A suitable test bench has been realized around the standard steering column of an A segment car as shown in Fig. 7. The IPMSM is connected to the steering column fully replacing the original DC Brushless machine, while a field oriented induction machine drive provides the load being connected to the front end of the steering column.

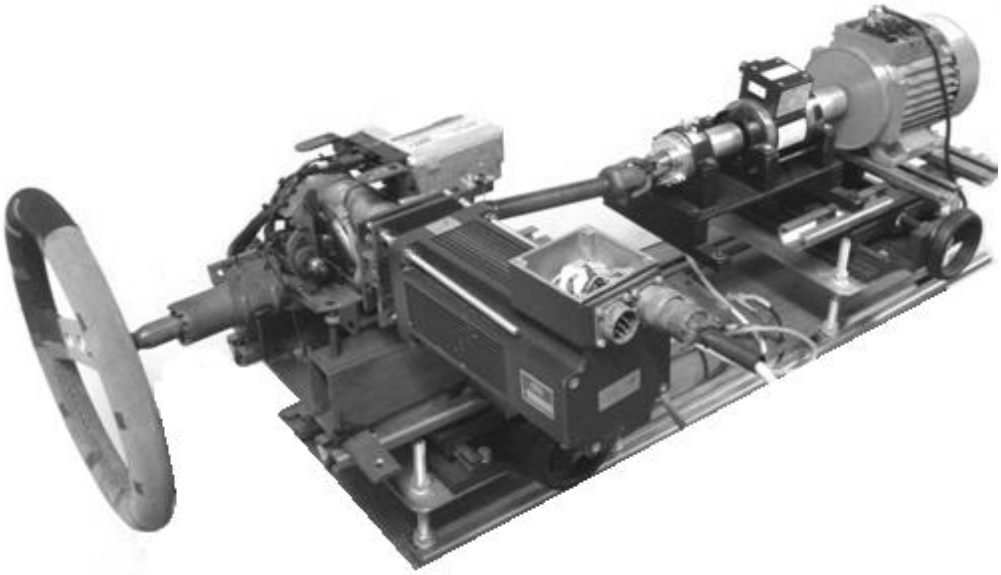

Fig. 7 – Experimental test bench.

A set of tests was performed on the experimental system to evaluate the robustness and accuracy of rotor position estimation. In Figs. 8 and 9 the estimated angular position is compared with a direct position measurement obtained with a resolver. In these tests the machine rotates at no load at *3 rad/s*, and *150 rad/s*. Tests at the same speed levels he were also performed under rated torque conditions, as shown in Figs. 10 and 11. It can be noticed that at a higher speed the estimation error increases, however is always limited at less than *9* electrical degrees. Finally, a very critical low speed reversal is shown in Fig. 12. In this case the machine smoothly responds to a sudden reference speed variation from *-10 rad/s* to *10 rad/s*.

The speed feedback signal has been obtained from the estimated rotor position using a state observer.

A major role in correctly estimating the rotor position is played by the amplitude and frequency of V_{shf}. Low V_{shf} values, in fact, prevent a precise detection of the rotor position, due to noises and measurement errors. On the other hand, high V_{shf} would generate unacceptable extra noises and losses. In the present case, V_{shf} has been settled to *11V (0.07 p.u.)* by trials, obtaining an experimentally evaluated efficiency reduction of less than *1%* at rated power. Also the selection of the frequency of the injected signal is a key point to ensure a precise estimation, especially at high speed. In the experimental tests shown the injected frequency was set to *500Hz* but trials at *1200 Hz* have been also successfully performed. Of course, by increasing the frequency the amplitude of the injected signal V_{shf} must be also suitably increased, affecting the power losses. Additional losses at *1200 Hz* have been experimentally evaluated as *3%* of the total losses.

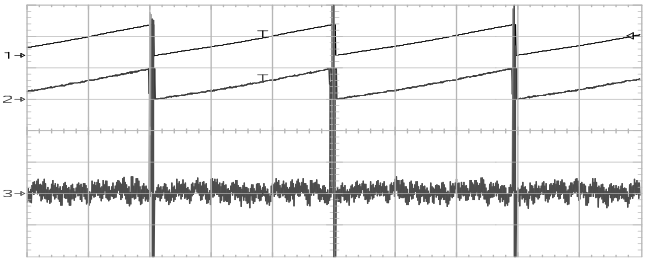

Fig. 8 No –load ω_r=*3rad/s – Time = 400 ms/div*;
1) Measured rotor position *[2π rad/div]*,
2) Estimated rotor position *[2π rad/div]*,
3) Estimation error *[(π/20)/div]*.

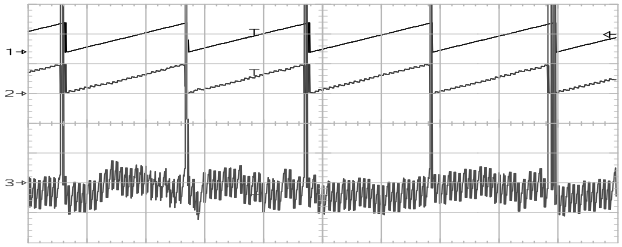

Fig. 9 No –load ω_r=150rad/s – Time = 10 ms/div; 1) Measured rotor position *[2π rad/div]*, 2) Estimated rotor position *[2π rad/div]*, 3) Estimation error *[(π/20)/div]*.

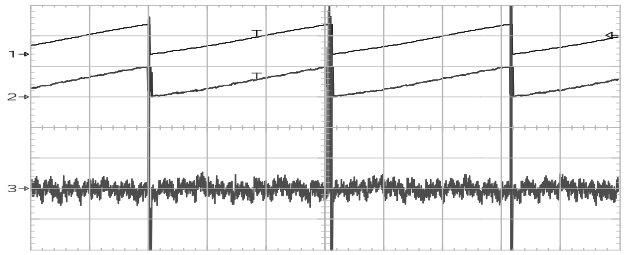

Fig. 10 Rated –load ω_r=3rad/s – Time = 400 ms/div; 1) Measured rotor position *[2π rad/div]*, 2) Estimated rotor position *[2π rad/div]*, 3) Estimation error *[(π/20)/div]*.

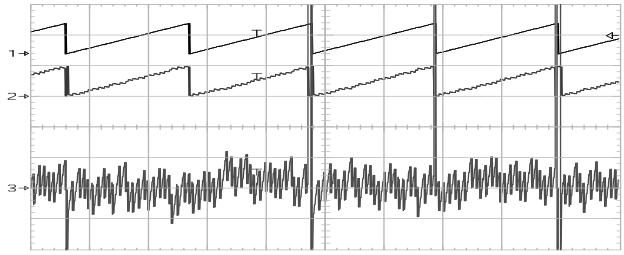

Fig. 11 Rated –load ω_r=150rad/s – Time = 10 ms/div; 1) Measured rotor position *[2π rad/div]*, 2) Estimated rotor position *[2π rad/div]*, 3) Estimation error *[(π/20)/div]*.

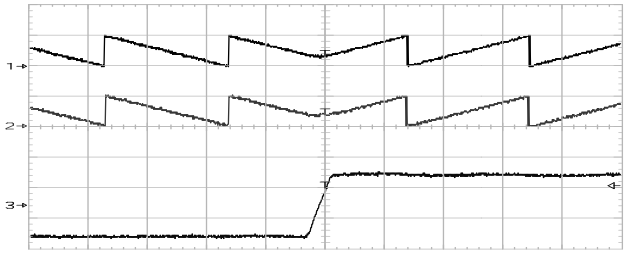

Fig. 12 - No –load speed transient ω_r=±10rad/s – Time = 100 ms/div; 1) 2) *[2*π rad /div]*, 3) *[10 rad/s/div]*.

5 Conclusion

A simple sensorless control of an IPMS machine, has been presented that can be almost completely implemented through an analog circuitry. This is a distinctive advantage in automotive electronic applications, where the cost is the most critical parameter of any new design. Thanks to the possibility to implement a large part of the control scheme through analog circuits, standard low end microprocessors, yet equipping DC brushless power steering systems, can be used to realize a sensorless IPMSM based EPS system. The proposed sensorless technique taking advantage from the injection of a high frequency voltage signal, does not require the knowledge of any motor parameter and is insensitive to parameters variation. Practical implementation issues have been deeply examined. Moreover, experimental results obtained on a standard electric power steering system in practical working conditions, have been presented, confirming the consistence of the proposed approach.

References:

[1] N. Bianchi, S. Bolognani, M. Dai Prè,; M. Tomasini, L. Peretti, M. Zigliotto, "The steering effect PM motor drives for automotive systems", IEEE Industry Applications Magazine, vol. 14, n. 2, March-April 2008, pp. 40-48.

[2] B.S. Bhangu, C.M.Bingham, "GA-tuning of nonlinear observers for sensorless control of automotive power steering IPMSMs", proceeding of IEEE Conference on Vehicle Power and Propulsion, 2005, 7-9 September, pp. 772-779

[3] S. Mir, M. Islam, and T. Sebastian, ''Role of electronics and controls in steering system,'' in Rec. 29th IEEE Annu. Conf. IEEE Industrial Electronics Society, Roanoke, 2003, pp. 2859–2864

[4] A. Consoli, G. Scarcella; G. Scelba, A. Testa, S. De Caro, "Sensorless IPMS motor drive control for electric power steering," Power Electronics Specialists Conference, 2008. PESC 2008. IEEE , pp.1488-1494, 15-19 June 2008.

[5] A. Consoli, G. Scarcella, A. Testa, "Industry Application of Zero-Speed Sensorless Control Techniques for PM Synchronous Motors", IEEE Transactions on Industry Applications, vol. 37, n.2, March-April 2002, pp. 513-520.

[6] Jung-Ik Ha, K. Ide, T. Sawa, Seung-Ki Sul, "Sensorless position control and initial position estimation of an interior permanent magnet motor", proceeding of IEEE IAS Annual Meeting, 2001, 30 September-4 October, pp. 2607-2613.
[7] Kim Hyunbae, R.D. Lorenz, "Carrier signal injection based sensorless control methods for IPM synchronous machine drives", proceeding of IEEE IAS Annual Meeting, 2004, 3-7 October, pp. 977-984.
[8] A. Consoli, G. Scarcella, G. Scelba, A. Testa, D. A. Triolo, "Sensorless Rotor Position Estimation in Synchronous Reluctance Motors Exploiting a Flux Deviation Approach", IEEE Transactions on Industry Applications, vol. 43, n.5, Sept.-Oct. 2007, pp. 1266-1273.
[9] P. Guglielmi, M. Pastorelli, G. Pellegrino, A. Vagati, "Position-sensorless control of permanent-magnet-assisted synchronous reluctance motor", IEEE Transactions on Industry Applications, vol. 40, n. 2, March-April 2004, pp. 615-622.
[10] J. Holtz, "Initial Rotor Polarity Detection and Sensorless Control of PM Synchronous Machines", proceeding of IEEE IAS Annual Meeting, 2006, 8-12 October, pp. 2040-2047.
[11] Kim Hyunbae, Huh Kum-Kang, R.D. Lorenz, T.M. Jahns, "A novel method for initial rotor position estimation for IPM synchronous machine drives", IEEE Transactions on Industry Applications, vol. 40, n.5, Sept.-Oct. 2004, pp. 1369-1378.
[12] G. Ombach, J. Junak, "Two rotors designs' comparison of permanent magnet brushless synchronous motor for an electric power steering application", European Conference on Power Electronics and Applications, 2007, 2-5 September, pp. 1-9.